

Dietary Supplementation of Inulin On Glycolipid Metabolism in Gestational Diabetes Mellitus via RENT/AKT/IRS Pathway

Miao Miao

Nanjing Maternity and Child Health Care Hospital <https://orcid.org/0000-0002-3952-6451>

Yongmei Dai

Nanjing Maternity and Child Health Care Hospital

Can Rui

Nanjing Maternity and Child Health Care Hospital

Yuru Fan

Nanjing Maternity and Child Health Care Hospital

Xinyan Wang

Nanjing Maternity and Child Health Care Hospital

Chong Fan

Nanjing Maternity and Child Health Care Hospital

Juan Mu

Nanjing Maternity and Child Health Care Hospital

Wenwen Hou

Nanjing Maternity and Child Health Care Hospital

Zhiyong Dong

Nanjing Maternity and Child Health Care Hospital

Ping Li

nanjing maternity and child health care hospital

Guiju Sun

Southeast University

Xin Zeng (✉ august555482@126.com)

Nanjing Maternity and Child Health Care Hospital <https://orcid.org/0000-0001-9872-7918>

Research

Keywords: Gestational diabetes, Fasting blood glucose, Inulin, Glycolysis/gluconeogenesis pathway, RETN

Posted Date: September 17th, 2021

DOI: <https://doi.org/10.21203/rs.3.rs-818583/v1>

License:  This work is licensed under a Creative Commons Attribution 4.0 International License.

[Read Full License](#)

Abstract

Background: Gestational diabetes mellitus (GDM) has significant short and long-term health consequences for both the mother and child. There is limited but suggestive evidence that inulin could improve glucose tolerance during pregnancy. This study assessed the effect of inulin on glucose homeostasis and elucidated the molecular mechanisms underlying the inulin-induced antidiabetic effects during pregnancy.

Method: Female C57BL/6 mice were randomized to receive either no treatment, high-dose inulin and low-dose inulin for 7 weeks with measurement of biochemical profiles. A real-time² (RT²) profiler polymerase chain reaction (PCR) array involved in glycolipid metabolism was measured.

Results: Inulin treatment facilitated glucose homeostasis in a dose-dependent manner by decreasing fasting blood glucose and total cholesterol, and improving glucose tolerance. Suppressing resistin (RETN) expression was observed in the inulin treatment group and the expression was significantly correlated with fasting blood glucose levels. The ratios of p-IRS to IRS and p-Akt to Akt in liver tissue and the ratio of p-Akt to Akt in adipose tissue increased significantly after inulin treatment.

Conclusions: Our findings indicated the observed decreased glucose level may be due to insulin signaling pathway repairment due to decreased expression of RETN and enhanced phosphorylation of IRS and Akt in GDM mice.

Introduction

Gestational diabetes mellitus (GDM)-defined as hyperglycemia, insulin resistance, and carbohydrate intolerance with the onset or first recognition during pregnancy-is a common obstetric complication, affecting an estimated 15.8% of pregnancies worldwide[1, 2]. GDM women have an increased risk of adverse maternal and perinatal complications, including preeclampsia, hydramnios, increased operative intervention and future type 2 diabetes mellitus, macrosomia [3, 4], congenital anomalies, metabolic abnormalities [5–9], and subsequent childhood and adolescent obesity [10]. In addition, increased levels of inflammatory mediators and biomarkers of oxidative stress can induce maternal insulin resistance, DNA damage, and chromosomal aberrations [11, 12].

This perpetuates an intergenerational cycle of disease that further escalates the obesity epidemic. To break this cycle, it would be beneficial to generate therapies that prevent GDM from developing [13]. Current treatments include diet and lifestyle interventions, followed by insulin treatment and, in some countries, oral agents such as metformin. Although women are able to maintain adequate glycemic control using these treatment strategies, they can be difficult to implement, and concerns remain regarding the long-term effects of oral agents on the developing fetus. For these reasons, it would be beneficial to develop novel, safe, and effective strategies for GDM risk reduction [14].

Inulin is a soluble dietary fiber, which is stored in the tubers of a perennial herb Jerusalem artichoke [15, 16]. Due to the specific chemical structure, inulin dietary fiber is not digested in the human mouth, stomach, or small intestine, so that it does not cause increase in blood glucose concentration, but rather prevents sharp changes in blood sugar and protecting islet cells after ingestion, thus known as “natural insulin” for diabetic patients [17]. In 2017, a systematic review of clinical trial results showed that dietary supplementation with inulin reduced biomarkers of metabolic syndrome [18]. In the United States in 2018, the Food and Drug Administration approved inulin as a dietary fiber ingredient used to improve the nutritional value of manufactured food products. Inulin-treated hyperglycemic mice had decreased average daily food consumption, body weight, average daily water consumption and relative liver weight and blood concentrations of TAG, total cholesterol, HDL-cholesterol and fasting blood glucose [19].

Furthermore, inulin has been associated with improved glucose metabolism and reduced risk of GDM [20]. While the mechanisms linking inulin to metabolic health are poorly understood, inulin are known to modify the intestinal microbiome and stimulate production of short-chain fatty acids (SCFAs). SCFAs affect the expression of a number of proteins that have been demonstrated to decrease gut permeability and increase insulin sensitivity [21, 22]. However, the evidence that inulin supplementation should be recommended before or during pregnancy to reduce the risk of GDM is limited [23, 24]. This study was, therefore, carried out to investigate the mechanism and effects of inulin supplementation on glycolipid metabolism and pregnancy outcomes in GDM mice.

Materials And Methods

Animals and Study Design

Six to seven-week-old C57BL/6J mice were purchased from Vital River Laboratory Animal Technology Co., Ltd., (China) and acclimatized to the animal facility for 1 week. Mice were maintained on a 12-h light-dark cycle with free access to food and water. All experiments were performed in accordance with the Animals (Scientific Procedures) Act 1986 and approved by the Ethics Committee of Women’s Hospital of Nanjing Medical University (No.2018-49).

Female mice were fed normal chow diet (NCD group, Research Diets AIN-93G, consisting of 20.3 % protein, 63.9 % carbohydrate, and 15.8 % fat), a high-fat/sucrose diet (HFD) (GDM group, Research Diets D12451, consisting of 19.8% protein, 35.2 % carbohydrate, and 45% fat), high-dose inulin supplemented a high-fat/sucrose diet (Inulin-H group, 3.33g/kg/d via oral gavage) or low-dose inulin supplemented a high-fat/sucrose diet (Inulin-L group, 1.67g/kg/d via oral gavage) for 4 weeks before being mated with age-matched male mice. Upon identification of a copulatory plug, considered to be day 0 of pregnancy (GD0). Mice were euthanized by CO₂ inhalation on GD18 (or equivalent) after fasting for 6 hours from 8 AM and blood and tissues were collected. Liver and inguinal fat was quickly collected and kept at -80 °C.

Measurement of Body Weight, Blood Glucose and Serum Insulin

Body weight, blood glucose and serum insulin were monitored at different time points, including before dietary intervention, after 4 weeks of HFD, and on GD 0, 10, 14 and 18. Blood glucose and insulin levels were determined from tail venipuncture blood samples. Blood glucose concentration was measured immediately using a blood glucose meter and strips (Roche Accu-Chek Active, Mannheim, Germany). The blood samples were then centrifuged at low speed (4°C, 3000 rpm, 15 mins) within 1 hour, the supernatant was harvested and stored at -80°C for measuring serum insulin level by enzyme linked immune sorbent assay (ELISA; NJJC BIO Co., Ltd, Nanjing, China) according to the manufacturer's instructions. The homeostasis model assessment of insulin resistance (HOMA-IR) was calculated by the following formula: fasting blood glucose (FBG, mmol/L) × fasting serum insulin (μIU/mL) / 22.5. In addition, urine volume and fluid intake were observed daily.

Oral Glucose Tolerance Test

Glucose tolerance was determined by an oral glucose tolerance test (OGTT) on GD 14. Mice were fasted for 6 hours with free access to water and received an oral gavage of 20% D-glucose (2 g/kg body weight). Blood samples were collected from the tail vein at 0, 30, 60, 90 and 120 mins after glucose administration. Blood glucose levels were measured instantly using methods as mentioned above. Meanwhile, area under the curve (AUC) of blood glucose was calculated [25].

Serum Lipid Measurement

Levels of serum triglycerides (TG), total cholesterol (TC), low-density lipoprotein (LDL) and high-density lipoprotein (HDL) were measured using commercial kits (NJJC BIO Co., Ltd, Nanjing, China).

Haematoxylin-eosin Staining

Liver and inguinal fat tissues were fixed in 4% paraformaldehyde, decalcified, paraffin-embedded and stored at 4°C. After tissues were sliced into 4 μm sections, haematoxylin-eosin staining was performed. First, sections were stained with haematoxylin for 5–10 minutes, immersed in 70% ethanol for 30 minutes to remove cytoplasm colouring, alkalized with alkaline solution and washed with distilled water for 1 minute. Second, sections were stained with eosin for 30–60 seconds, dehydrated with gradient ethanol, cleared two times with xylene, dried and mounted. Finally, the morphological structures of the liver and inguinal fat tissues were observed under an optical microscope.

RT² Profiler PCR Array Analysis

Total RNA was isolated from the liver samples of NCD group, GDM group and Inulin-H group using Qiagen RNeasy® Mini Kit (QIAGEN, Shanghai, China) according to the manufacturer's instructions. Single-strand cDNA was synthesized from 1 μg of total RNA by reverse transcription reaction using Qiagen RT² First Strand Kit (QIAGEN, Shanghai, China). The cDNA was mixed with Qiagen PCR RT² SYBR Green Master Mix (QIAGEN, Shanghai, China).

To explore the underlying mechanisms of inulin induced-effects, the expression of 84 genes involved in Glycolipid metabolism including RETN were examined using RT² profiler PCR array (PAMM-006Z-mouse

glucose metabolism, QIAGEN, Shanghai, China). Relative quantification of mRNA levels was determined by real-time quantitative PCR using a ABI 7500 RT-PCR machine/Bio-Rad CFX96 Sequence Detector instrument. The quantitative expression of gene was calculated from the cycle threshold (CT) value of each sample in the linear part of the curve using the relative quantification method ($2^{-\Delta\Delta CT}$) [26]. The samples were analyzed in triplicate and corrected for the selected internal standard which had the smallest standard deviation among the housekeeping genes. Candidate genes were selected from those whose expressions differed greater than 2-fold or less than 2-fold, or which differed significantly ($p < 0.05$) between the GDM group and Inulin-H treatment group.

Quantitative PCR (qPCR) Analysis for the Candidate genes

The five most differentially-expressed genes between GDM group and Inulin-H group were selected from the RT² profiler PCR array as candidate genes and were analyzed the correlation with FBG further. Specific PCR primers were designed for further quantitative real-time PCR analysis (Takara, Dalian, China) as follows.

G6pc: 5'-CGACTCGCTATCTCCAAGTGA-3' and 5'-GGGCGTTGTCCAAACAGAAT-3'

RETN: 5'-ACAAGACTTCAACTCCCTGTTT-3' and 5'-TTTCTTCACGAATGTCCCACG-3'

Igfbp5: 5'-CCCTGCGACGAGAAAGCTC-3' and 5'-GCTCTTTTCGTTGAGGCAAACC-3'

Slc14a2: 5'-AAGGAGATGTCTGACAGCAACA-3' and 5'-GGGCTGGGTGTGTATCCTG-3'

IL10: 5'-CCCATTCTCGTCACGATCTC-3' and 5'-TCAGACTGGTTTGGGATAGGTTT-3'

Western Blot Analysis

Liver and inguinal fat tissues were harvested and were homogenized on ice in the presence of protease and phosphatase inhibitors. Homogenates were centrifuged at 12,000 × g at 4°C for 15 mins. Protein concentration in supernatants was quantified by the BCA method using bovine serum albumin (BSA) as the standard. Proteins were analyzed by 10% SDS-PAGE and transferred to PVDF membranes that were incubated in 5% non-fat milk at room temperature for 1 hr, then incubated with appropriate primary and secondary antibodies. Membranes were washed and proteins were detected by enhanced chemiluminescence (ECL) using a LAS-4000 lumino-image analyzer (Fuji Film, Tokyo, Japan). Bands were digitally scanned and analyzed using ImageJ software (NIH Image, National Institutes of Health, Bethesda, MD, USA).

Statistical Analysis

All data were calculated as means ± SD and checked using the Kolmogorov-Smirnov (KS) test before further analysis. Statistical significance between two datasets was assessed using the Student's t-test. Multiple groups were compared using one-way ANOVA followed by Tukey multiple comparison testing. A *P* value of < 0.05 was considered statistically significant. All statistical tests were performed using GraphPad Prism Version 7.0 (GraphPad Prism Software, Inc. CA, USA).

Result

Changes of Body Weight and Reproductive Outcome of Pregnant Mice

Body weight was determined at different time points for all groups. As indicated in Fig. 1A, the body weight of GDM group showed an increasing trend after 4 weeks of HFD prior to mating, and a rapid elevation of body weight was found in the mice of GDM group compared to the moderate increase in NCD group and Inulin-H group during peripartum. The weight at GD 18 and total weight gain of GDM (37.88 ± 3.32 g and 15.32 ± 0.86 g) and Inulin-L group (36.28 ± 3.16 g and 14.39 ± 0.97 g) were significantly higher than that of NCD group (34.54 ± 2.42 g and 13.13 ± 0.78 g) and Inulin-H group (33.34 ± 3.80 g and 12.22 ± 0.92 g) (Fig. 1B). After inulin intervention, the Inulin-H group showed no statistically significant difference in body weight compared with the NCD group (Fig. 1A and B). In addition, the urine volume and fluid intake were increased significantly during mid-to-late pregnancy in GDM mice compared to NCD mice. However, there was no significant change in the mice of Inulin-L or Inulin-H group.

The number, body weight and length of fetal mice in each group were compared. There was no significant difference in the number of fetal mice among groups (Fig. 1C). The average body weight and length of fetal mice born by GDM mothers (1.27 ± 0.17 g and 2.32 ± 0.08 cm) were significantly higher than those by NCD (0.94 ± 0.16 g and 2.23 ± 0.12 cm) and Inulin-H mothers (1.04 ± 0.07 g and 2.19 ± 0.10 cm) (Fig. 1D and E).

Blood Glucose, Serum Insulin and Glucose Tolerance Test in Mice

We examined the blood glucose and serum insulin in these mice. Blood glucose levels did not differ amongst the groups at the end of 4-week feeding before mating and exhibited a gradual upregulation during pregnancy in the mice of GDM and Inulin-L groups but not NCD or Inulin-H group (Fig. 2A). Moreover, blood glucose and serum insulin on GD 18 were significantly advanced in GDM mice (10.83 ± 0.93 mmol/l and 19.34 ± 1.98 mIU/L) in contrast to the NCD mice (8.77 ± 0.75 mmol/l and 13.52 ± 1.68 mIU/L) (Fig. 2B and D). Interestingly, blood glucose levels were deregulated at the end of pregnancy in each group (Fig. 2A), whereas insulin levels were increased in both GDM and Inulin-L mice and showed a more pronounced enhancement in the mice of GDM group (Fig. 2C). After inulin intervention, the Inulin-H group showed no statistically significant difference in blood glucose and insulin changes compared with the NCD group (Fig. 2A and C).

By performing a glucose tolerance test at the end of 4-week feeding before mating, we found that blood glucose and insulin levels of mice in GDM group indicated a slight increase without statistically significant differences, suggesting HFD for 4 weeks did not cause dramatical changes in either glucose or insulin levels (Fig. 2E and F). Then, we conducted the same test on GD 14. As shown in Fig. 2G, compared with NCD group, the mice in GDM group showed impaired glucose tolerance, as manifested by obviously

increased glucose levels after glucose injection ($P < 0.01$, 0, 30, 60, 90 and 120 mins). While the blood glucose of Inulin-L and Inulin-H group mice were dramatically lower than those of GDM group throughout the test ($P < 0.01$, Fig. 2G), as were the AUCs (Fig. 2H). All these suggested that inulin treatment could significantly improve the glucose tolerance of GDM mice.

Effects of Inulin on Lipid Profiles and Tissues Morphology in Mice

The levels of TG, TG and LDL in GDM group were significantly higher than those in the other three groups, suggesting that HFD could elevate serum lipid levels of GDM mice, while inulin intervention could significantly reduce serum triglyceride, total cholesterol and low-density lipoprotein levels of GDM mice (Fig. 3A, B and D). However, there was no significant difference in serum HDL among groups (Fig. 3C).

This finding was supported by histology, which showed an increase in lipid droplets in hepatic and adipose tissues from mice fed the HFD diet and the HFD diet supplemented with inulin compared to NCD. Hepatic lipid droplets and adipocyte hypertrophy were significantly alleviated in mice from Inulin-L and Inulin-H group compared to GDM group (Fig. 3E), suggesting that inulin could attenuate the fat accumulation induced by HFD.

Effects of Inulin on the Expression of those Genes Involved in Glycolipid Metabolism Pathway

Sixteen genes involved in the glycolipid metabolism were detected with different expressions between Inulin-H group mice and GDM mice in hepatic tissues. (Fig. 4A-C). The five most differentially-expressed genes (G6pc, Slc14a2, Igfbp5, RETN, Il10) were validated by qPCR with the specific primers in hepatic and adipose tissues. We found that the 5 five genes' expressions were consistent with RT² profiler PCR array results, and the consistent results were observed on the housekeeping genes as well. In particular, the expression of RETN was significantly down-regulated after inulin treatment compared to GDM in hepatic (1.10 ± 0.01 VS 4.30 ± 0.60) (Fig. 4D) and adipose tissues (1.17 ± 0.01 VS 15.86 ± 2.10) (Fig. 4E). We next examined the association between RETN relative expression in hepatic and adipose tissues and FBG levels on GD18. We found that increased RETN expression was significantly correlated with increasing fasting glucose (Fig. 4F and G).

Measurement of alterations of protein expression by western blotting

Previous studies have shown that RETN played an important role in the regulation of insulin signaling pathway. RETN could induce insulin resistance by inhibiting the phosphorylation of IRS, Akt and ERK 1/2 proteins [27].

Western blotting was used to investigate any changes of RETN and these kinases (IRS, Akt and ERK 1/2) after inulin treatment in mouse liver and adipose tissue. The western blot analysis results showed that the protein level of RETN was consistent with the mRNA results (Fig. 5A-C). The ratio of p-IRS to IRS

signal molecule in liver tissue of GDM group was significantly reduced compared to NCD group (Fig. 6A and B). After the ITF-H treatment, the ratios of p-IRS to IRS and p-Akt to Akt in liver tissue and the ratio of p-Akt to Akt in adipose tissue increased significantly (Fig. 6A and C). These results suggested that inulin could enhance the phosphorylation of IRS and Akt signaling molecules to improve glucose and lipid metabolism in GDM mice.

Discussion

The recommended diet for glycemic control should be rich in dietary fiber [28]. Inulin is a widely distributed carbohydrate in nature, which is a recognized dietary fiber [29]. In the present study, inulin improved glucose tolerance, reduced insulin resistance, and lowered body weight, serum triglyceride, total cholesterol and low-density lipoprotein levels in GDM mice. Moreover, inulin improved the pregnancy outcomes of GDM mice. In addition, a further significant decrease of RETN expression and increase of the phosphorylation level of IRS and Akt signaling molecules in insulin signaling pathway were observed upon exposure to inulin. Taken together, our study demonstrates a beneficial effect of inulin in the control of gestational diabetes, and this effect is related to the activation of insulin signaling pathway.

GDM is a metabolic disorder that is characterized by hyperglycemia accompanied with insulin resistance. In the present study, the blood glucose level and insulin level were significantly increased in the GDM group mice on GD 18, indicating that GDM was successfully established in these animals [30, 31]. We also observed disorders of lipid metabolism in GDM mice as evidenced by elevated serum levels of TG, TC and LDL, which is similar to the metabolic profile in the humans with GDM [32]. The therapeutic effects of inulin on metabolic disorders have been extensively reported [33–35]. A previous study showed that oral administration of inulin at 5 g/kg/day for 10 weeks protected the rats from diabetes-induced renal injury [36]. In the present study, we chose the doses of 3.33 and 1.67 g/kg/day to evaluate the potential antidiabetic effects of inulin in mice. The results showed that 4 weeks before mating and throughout pregnancy treatment with inulin relieved the diabetic symptoms as evidenced by reduced blood glucose level and insulin level. However, Farhangi et al. found that inulin significantly reduced the fasting serum glucose level and HbA1C ratio, but had little effect on the insulin level in patients with T2DM [37]. Our results showed that inulin modulated glucose metabolism in a dose-dependent manner, thus we speculate that the differential effects of inulin on insulin may be due to different dosages (10g/day for T2DM patients in Farhangi et al.'s study). Moreover, we observed a strong hypolipidemic effect of inulin in GDM rats. These results agree with a previous study showing that inulin promoted lipid metabolism by altering the expression of acetyl-CoA carboxylase and the activities of fatty acid synthase and xanthine oxidase [34].

Liver and adipose are major contributors that responsible for lipid and glucose metabolism, and they are sensitive to insulin signal for the regulation of glucose homeostasis [38]. In the pathological conditions of GDM, insulin action is compromised and glucose uptake by these cells were disrupted, resulting in hyperglycemia [39, 40]. In the present study, treatment with chicory inulin could attenuate increased lipid droplet size in retroperitoneal fat tissue and hepatic lipid accumulation induced by HFD.

To explore the underlying mechanisms of inulin induced antidiabetic effects, the expression of 84 genes involved in glucose metabolism were examined. Five candidate genes with most differential-expression following inulin treatment were validated, and they were mainly involved in the glycolysis/gluconeogenesis pathway and participated in different types of metabolism process including glucose metabolic process and gluconeogenesis. Insulin signaling plays a pivotal role in maintaining basic cellular functions such as synthesis and degradation of glycogen, lipids and proteins [41]. In this study, we found that RETN expression was the most down-regulated after inulin treatment, and this down-regulation was positive correlated with fasting glucose level in GDM mice. RETN is a pro-inflammatory adipokine that as an influential factor interferes with insulin action, signaling, and glucose metabolism [41–44]. Benomar et al. demonstrated that RETN interfered with normal insulin signaling pathway by inhibiting phosphorylation of IRS, Akt, and ERK 1/2 [27]. In this present study, the ratios of p-IRS to IRS and p-Akt to Akt in liver tissue and the ratio of p-Akt to Akt in adipose tissue increased significantly after the inulin treatment. This indicated the observed decreased glucose level may be due to insulin signaling pathway repairment due to decreased expression of RETN and enhanced phosphorylation of IRS and Akt in GDM mice.

In addition to RETN and insulin signaling pathway, some other genes and signaling pathways are also implicated in the regulation of glucolipid metabolism, such as AMP-activated protein kinase (AMPK) and PI3K/AKT pathways [45, 46]. Exploring whether exerts its glucose-control effects through these pathways, though beyond the scope of our present study, will provide interesting insights into the molecular mechanisms underlying inulin's hypoglycemic action. Thus, further studies are needed to verify the involvement of other pathways in mediating the anti-diabetic actions of inulin.

Conclusions

In summary, our study demonstrates that inulin could lower blood glucose level and improve glucolipid metabolism, and it could also promote pregnancy outcomes in gestational diabetic mice. These actions are likely to be mediated via repairment of insulin signaling pathway. Our findings suggest a potential value of inulin as a healthcare supplement for GDM patients.

Abbreviations

GDM
Gestational diabetes mellitus; SCFAs:Short-chain fatty acids; NCD:Normal chow diet; HFD:High-fat/sucrose diet; FBG:Fasting blood glucose; IR:Insulin resistance; OGTT:Oral glucose tolerance test; AUC:Area under the curve; TG:Triglycerides; TC:Total cholesterol; LDL:Low-density lipoprotein; HDL:High-density lipoprotein; RETN:Resistin; IRS:Insulin receptor; Akt:Protein kinase B; ERK 1/2:Extracellular signal-regulated protein kinases 1 and 2.

Declarations

Ethics approval and consent to participate

The animal experiments were performed according to internationally followed ethical standards and approved by the Ethics Committee of Women's Hospital of Nanjing Medical University (No.2018-49).

Consent for publication

Not applicable.

Availability of data and materials

The datasets used and/or analyzed during the current study are available from the corresponding author upon reasonable request.

Competing interests

The authors declare no conflict of interest.

Funding

This work was supported by the National Natural Science Foundation of China (Grant Nos. 81801480), Six Talent Project in Jiangsu Province (WSY-119, WSW-120).

Author's Contributions

Miao Miao, Yongmei Dai, Ping Li, Guiju Sun and Xin Zeng designed the experiments; Can Rui and Chong Fan performed the experiments; Yuru Fan and Xinyan Wang analyzed the data; Juan Mu, Wenwen Hou and Zhiyong Dong contributed reagents/ materials/ analysis tools; Miao Miao wrote the paper.

Acknowledgements

Not applicable.

References

1. Association AD. 2. Classification and Diagnosis of Diabetes: Standards of Medical Care in Diabetes-2019. *Diabetes Care*. 2019;42:13-s28.
2. Saeedi P, Petersohn I, Salpea P, Malanda B, Karuranga S, Unwin N, Colagiuri S, Guariguata L, Motala AA, Ogurtsova K, et al: **Global and regional diabetes prevalence estimates for 2019 and projections for 2030 and 2045: Results from the International Diabetes Federation Diabetes Atlas, 9(th) edition.** *Diabetes Res Clin Pract* 2019, **157**:107843.
3. Martis R, Crowther CA, Shepherd E, Alsweiler J, Downie MR, Brown J. Treatments for women with gestational diabetes mellitus: an overview of Cochrane systematic reviews. *Cochrane Database Syst*

Rev. 2018;8:Cd012327.

4. Wendland EM, Torloni MR, Falavigna M, Trujillo J, Dode MA, Campos MA, Duncan BB, Schmidt MI. Gestational diabetes and pregnancy outcomes—a systematic review of the World Health Organization (WHO) and the International Association of Diabetes in Pregnancy Study Groups (IADPSG) diagnostic criteria. *BMC Pregnancy Childbirth*. 2012;12:23.
5. Wroblewska-Seniuk K, Wender-Ozegowska E, Szczapa J. Long-term effects of diabetes during pregnancy on the offspring. *Pediatr Diabetes*. 2009;10:432–40.
6. Woo Baidal JA, Locks LM, Cheng ER, Blake-Lamb TL, Perkins ME, Taveras EM. Risk Factors for Childhood Obesity in the First 1,000 Days: A Systematic Review. *Am J Prev Med*. 2016;50:761–79.
7. Hammoud NM, Visser GHA, van Rossem L, Biesma DH, Wit JM, de Valk HW. Long-term BMI and growth profiles in offspring of women with gestational diabetes. *Diabetologia*. 2018;61:1037–45.
8. Appiah D, Schreiner PJ, Gunderson EP, Konety SH, Jacobs DR Jr, Nwabuo CC, Ebong IA, Whitham HK, Goff DC Jr, Lima JA, et al. Association of Gestational Diabetes Mellitus With Left Ventricular Structure and Function: The CARDIA Study. *Diabetes Care*. 2016;39:400–7.
9. Lowe WL Jr. **Hyperglycemia and Adverse Pregnancy Outcome Follow-up Study (HAPO FUS): Maternal Gestational Diabetes Mellitus and Childhood Glucose Metabolism**. 2019, 42:372–380.
10. Chiefari E, Arcidiacono B, Foti D, Brunetti A. Gestational diabetes mellitus: an updated overview. *J Endocrinol Invest*. 2017;40:899–909.
11. Lappas M. Activation of inflammasomes in adipose tissue of women with gestational diabetes. *Mol Cell Endocrinol*. 2014;382:74–83.
12. Toljic M, Egic A, Munjas J, Karadzov Orlic N, Milovanovic Z, Radenkovic A, Vuceljic J, Joksic I. Increased oxidative stress and cytokines-block micronucleus cytome assay parameters in pregnant women with gestational diabetes mellitus and gestational arterial hypertension. *Reprod Toxicol*. 2017;71:55–62.
13. Page KA, Buchanan TA. The vicious cycle of maternal diabetes and obesity: moving from "what" to "how" and "why". *J Pediatr*. 2011;158:872–3.
14. Plows JF, Ramos Nieves JM, Budin F, Mace K, Reynolds CM, Vickers MH, Silva-Zolezzi I, Baker PN, Stanley JL. The effects of myo-inositol and probiotic supplementation in a high-fat-fed preclinical model of glucose intolerance in pregnancy. *Br J Nutr*. 2020;123:516–28.
15. Petrovsky N, Cooper PD. Advax™, a novel microcrystalline polysaccharide particle engineered from delta inulin, provides robust adjuvant potency together with tolerability and safety. *Vaccine*. 2015;33:5920–6.
16. Shoaib M, Shehzad A, Omar M, Rakha A, Raza H, Sharif HR, Shakeel A, Ansari A, Niazi S. Inulin: Properties, health benefits and food applications. *Carbohydr Polym*. 2016;147:444–54.
17. Jackson KG, Taylor GR, Clohessy AM, Williams CM. The effect of the daily intake of inulin on fasting lipid, insulin and glucose concentrations in middle-aged men and women. *Br J Nutr*. 1999;82:23–30.

18. Liu F, Prabhakar M, Ju J, Long H, Zhou HW. Effect of inulin-type fructans on blood lipid profile and glucose level: a systematic review and meta-analysis of randomized controlled trials. *Eur J Clin Nutr.* 2017;71:9–20.
19. Shao T, Yu Q, Zhu T, Liu A, Gao X, Long X. **Inulin from Jerusalem artichoke tubers alleviates hyperglycaemia in high-fat-diet-induced diabetes mice through the intestinal microflora improvement.** 2020, 123:308–318.
20. Ahmadi S, Jamilian M, Tajabadi-Ebrahimi M, Jafari P, Asemi Z. The effects of synbiotic supplementation on markers of insulin metabolism and lipid profiles in gestational diabetes: a randomised, double-blind, placebo-controlled trial. *Br J Nutr.* 2016;116:1394–401.
21. Taylor BL, Woodfall GE, Sheedy KE, O'Riley ML, Rainbow KA, Bramwell EL, Kellow NJ. **Effect of Probiotics on Metabolic Outcomes in Pregnant Women with Gestational Diabetes: A Systematic Review and Meta-Analysis of Randomized Controlled Trials.** *Nutrients* 2017, 9.
22. Tilg H, Moschen AR. Food, immunity, and the microbiome. *Gastroenterology.* 2015;148:1107–19.
23. Rogozińska E, Chamillard M, Hitman GA, Khan KS, Thangaratinam S. Nutritional manipulation for the primary prevention of gestational diabetes mellitus: a meta-analysis of randomised studies. *PLoS One.* 2015;10:e0115526.
24. Plows JF, Reynolds CM, Vickers MH, Baker PN, Stanley JL. Nutritional Supplementation for the Prevention and/or Treatment of Gestational Diabetes Mellitus. *Curr Diab Rep.* 2019;19:73.
25. Torimoto K, Okada Y, Tanaka Y, Matsuoka A, Hirota Y, Ogawa W, Saisho Y, Kurihara I, Itoh H, Inada S, Koga M. Usefulness of the index calculated as the product of levels of fasting plasma glucose and hemoglobin A1c for insulinoma screening. *Endocr J.* 2020;67:509–13.
26. Livak KJ, Schmittgen TD. Analysis of relative gene expression data using real-time quantitative PCR and the 2^{(-Delta Delta C(T))} Method. *Methods.* 2001;25:402–8.
27. Benomar Y, Gertler A, De Lacy P, Crépin D, Ould Hamouda H, Riffault L, Taouis M. Central resistin overexposure induces insulin resistance through Toll-like receptor 4. *Diabetes.* 2013;62:102–14.
28. Weickert MO, Pfeiffer AFH. Impact of Dietary Fiber Consumption on Insulin Resistance and the Prevention of Type 2 Diabetes. *J Nutr.* 2018;148:7–12.
29. Cai X, Yu H, Liu L, Lu T, Li J, Ji Y, Le Z, Bao L, Ma W, Xiao R, Yang Y. Milk Powder Co-Supplemented with Inulin and Resistant Dextrin Improves Glycemic Control and Insulin Resistance in Elderly Type 2 Diabetes Mellitus: A 12-Week Randomized, Double-Blind, Placebo-Controlled Trial. *Mol Nutr Food Res.* 2018;62:e1800865.
30. Skovsø S. Modeling type 2 diabetes in rats using high fat diet and streptozotocin. *J Diabetes Investig.* 2014;5:349–58.
31. Islam MS, Loots du T. Experimental rodent models of type 2 diabetes: a review. *Methods Find Exp Clin Pharmacol.* 2009;31:249–61.
32. Benaicheta N, Labbaci FZ, Bouchenak M, Boukourt FO. Effect of sardine proteins on hyperglycaemia, hyperlipidaemia and lecithin:cholesterol acyltransferase activity, in high-fat diet-induced type 2 diabetic rats. *Br J Nutr.* 2016;115:6–13.

33. Lin W, Liu C, Yang H, Wang W, Ling W, Wang D. Chicory, a typical vegetable in Mediterranean diet, exerts a therapeutic role in established atherosclerosis in apolipoprotein E-deficient mice. *Mol Nutr Food Res*. 2015;59:1803–13.
34. Lin Z, Zhang B, Liu X, Jin R, Zhu W. Effects of chicory inulin on serum metabolites of uric acid, lipids, glucose, and abdominal fat deposition in quails induced by purine-rich diets. *J Med Food*. 2014;17:1214–21.
35. Nishimura M, Ohkawara T, Kanayama T, Kitagawa K, Nishimura H, Nishihira J. Effects of the extract from roasted chicory (*Cichorium intybus* L.) root containing inulin-type fructans on blood glucose, lipid metabolism, and fecal properties. *J Tradit Complement Med*. 2015;5:161–7.
36. Ning C, Wang X, Gao S, Mu J, Wang Y, Liu S, Zhu J, Meng X. **Chicory inulin ameliorates type 2 diabetes mellitus and suppresses JNK and MAPK pathways in vivo and in vitro.** *Mol Nutr Food Res* 2017, 61.
37. Farhangi MA, Javid AZ, Dehghan P. The effect of enriched chicory inulin on liver enzymes, calcium homeostasis and hematological parameters in patients with type 2 diabetes mellitus: A randomized placebo-controlled trial. *Prim Care Diabetes*. 2016;10:265–71.
38. Zhao W, Li A, Feng X, Hou T, Liu K, Liu B, Zhang N. Metformin and resveratrol ameliorate muscle insulin resistance through preventing lipolysis and inflammation in hypoxic adipose tissue. *Cell Signal*. 2016;28:1401–11.
39. Hajiaghaalipour F, Khalilpourfarshbafi M, Arya A. Modulation of glucose transporter protein by dietary flavonoids in type 2 diabetes mellitus. *Int J Biol Sci*. 2015;11:508–24.
40. Stanford KI, Goodyear LJ. Exercise and type 2 diabetes: molecular mechanisms regulating glucose uptake in skeletal muscle. *Adv Physiol Educ*. 2014;38:308–14.
41. Saltiel AR, Kahn CR. Insulin signalling and the regulation of glucose and lipid metabolism. *Nature*. 2001;414:799–806.
42. Benomar Y, Taouis M. Molecular Mechanisms Underlying Obesity-Induced Hypothalamic Inflammation and Insulin Resistance: Pivotal Role of Resistin/TLR4 Pathways. *Front Endocrinol (Lausanne)*. 2019;10:140.
43. Derosa G, Catena G, Gaudio G, D'Angelo A, Maffioli P. Adipose tissue dysfunction and metabolic disorders: Is it possible to predict who will develop type 2 diabetes mellitus? Role of markers in the progression of diabetes in obese patients (The RESISTIN trial). *Cytokine*. 2020;127:154947.
44. Nemes A, Homoki JR, Kiss R, Hegedűs C, Kovács D, Peitl B, Gál F, Stündl L, Szilvássy Z, Remenyik J: **Effect of Anthocyanin-Rich Tart Cherry Extract on Inflammatory Mediators and Adipokines Involved in Type 2 Diabetes in a High Fat Diet Induced Obesity Mouse Model.** *Nutrients* 2019, 11.
45. Wang S, Xu J, Song P, Viollet B, Zou MH. In vivo activation of AMP-activated protein kinase attenuates diabetes-enhanced degradation of GTP cyclohydrolase I. *Diabetes*. 2009;58:1893–901.
46. Dai B, Wu Q, Zeng C, Zhang J, Cao L, Xiao Z, Yang M. The effect of Liuwei Dihuang decoction on PI3K/Akt signaling pathway in liver of type 2 diabetes mellitus (T2DM) rats with insulin resistance. *J Ethnopharmacol*. 2016;192:382–9.

Figures

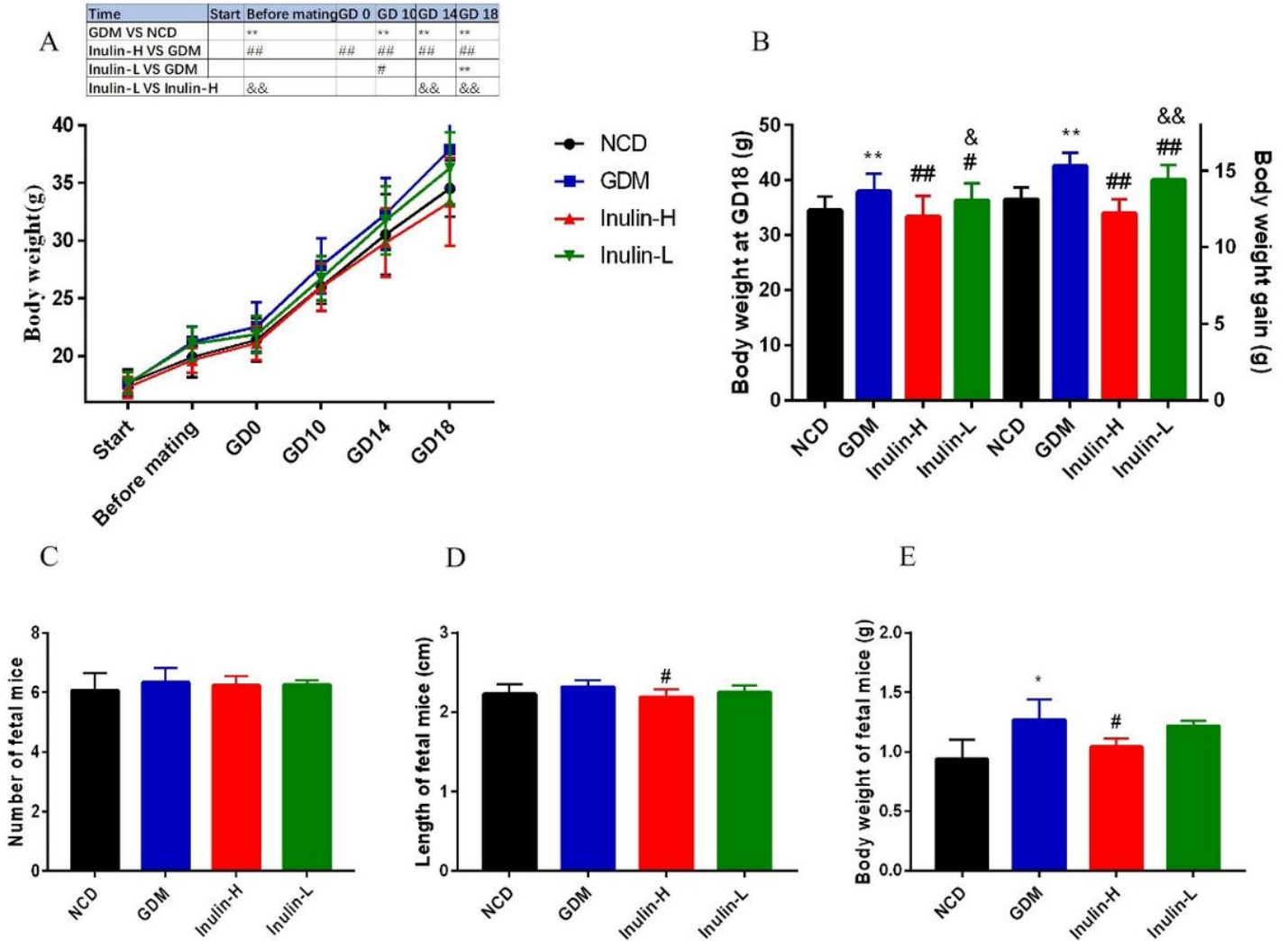


Figure 1

Changes of body weight (A, B), the number, length of fetal mice (C, D) and body weight at birth (E). Data are expressed as the mean \pm SD values (n = 15). *P < 0.05, **P < 0.01 vs NCD group; #P < 0.05, ##P < 0.01 vs GDM; &P < 0.05, &&P < 0.01 vs Inulin-H group.

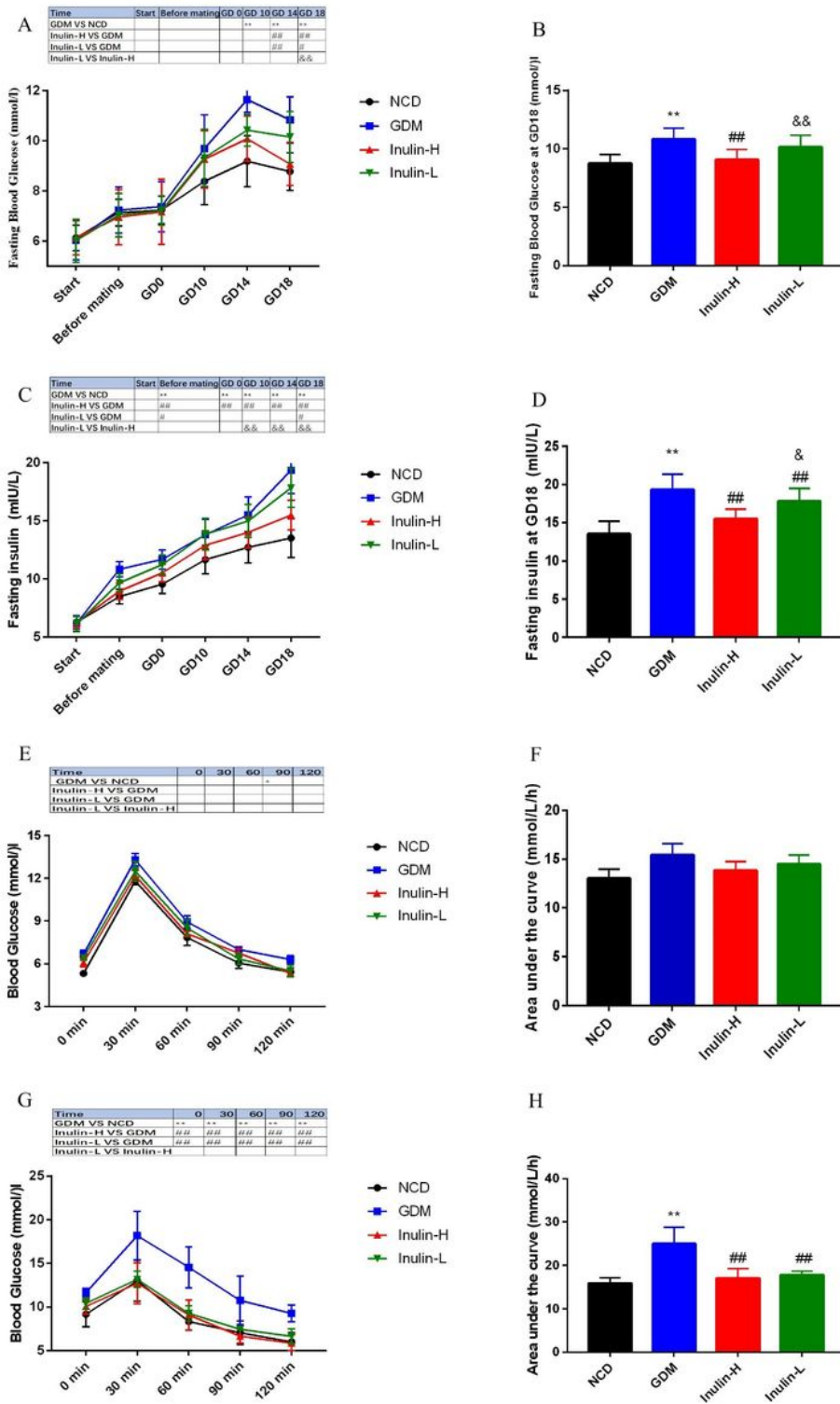


Figure 2

Changes of blood glucose (A, B), and serum insulin (C, D) in mice of different groups before dietary intervention, after 4 weeks of HFD, and on GD 0, 10, 14 and 18. Blood glucose (E, F) during oral glucose tolerance test in the four groups after 4 weeks of HFD. Blood glucose (C, D) during oral glucose tolerance test in the four groups on GD 14. Data are expressed as the mean \pm SD values ($n = 15$). ** $P < 0.01$ vs NCD group; ### $P < 0.01$ vs GDM; &# $P < 0.05$, && $P < 0.01$ vs Inulin-H group.

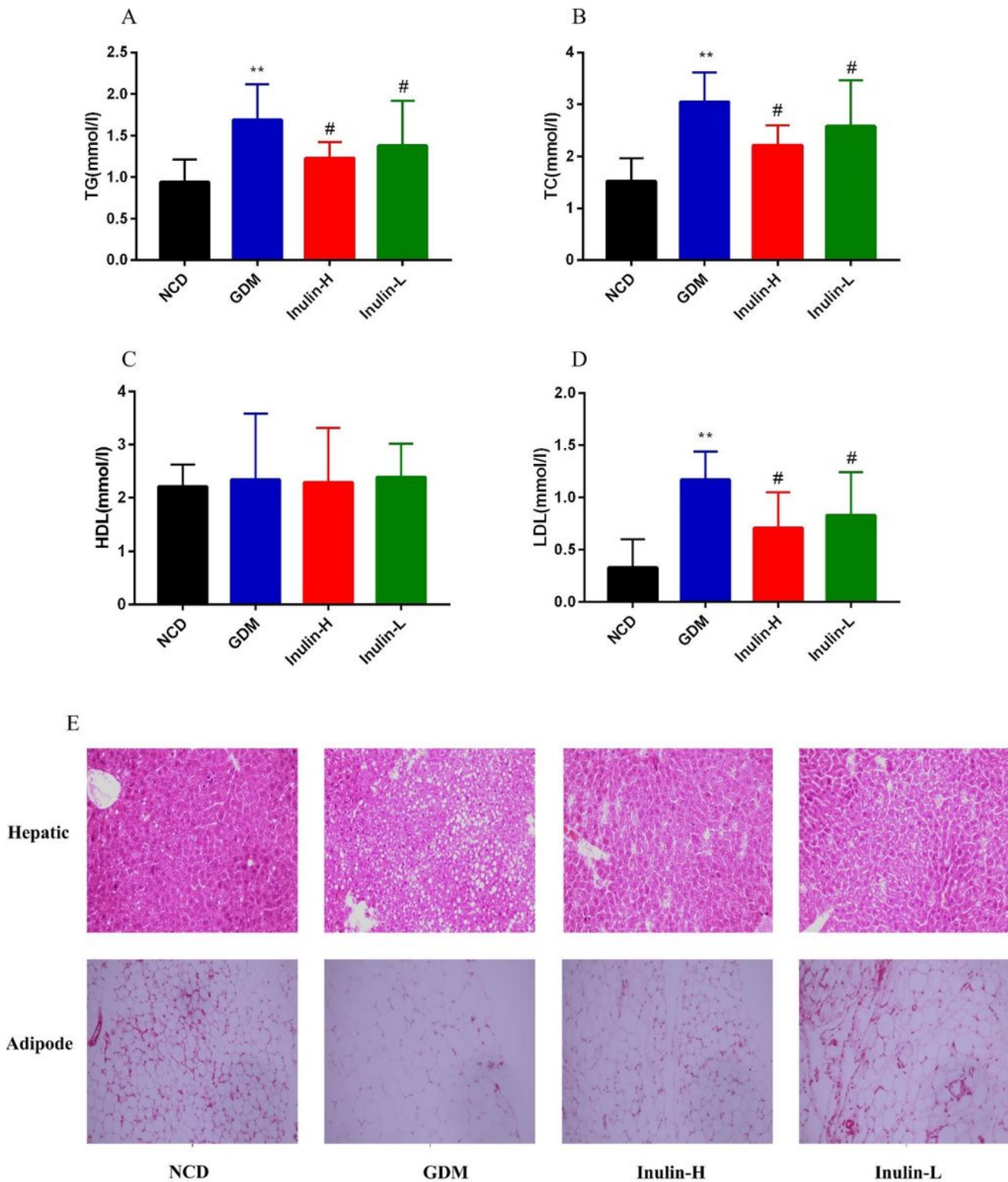


Figure 3

Changes of lipid profile (A-D) in mice of different groups GD 18. Data are expressed as the mean \pm SD values (n = 15). **P<0.01 vs NCD group; #P <0.05 vs GDM. Changes of hepatic and adipose morphology (E). The hepatic and adipose tissues were stained with HE for morphologic analysis under light microscopy. Morphologic changes of hepatic and adipose cells were observed under a high magnification field (\times 200)

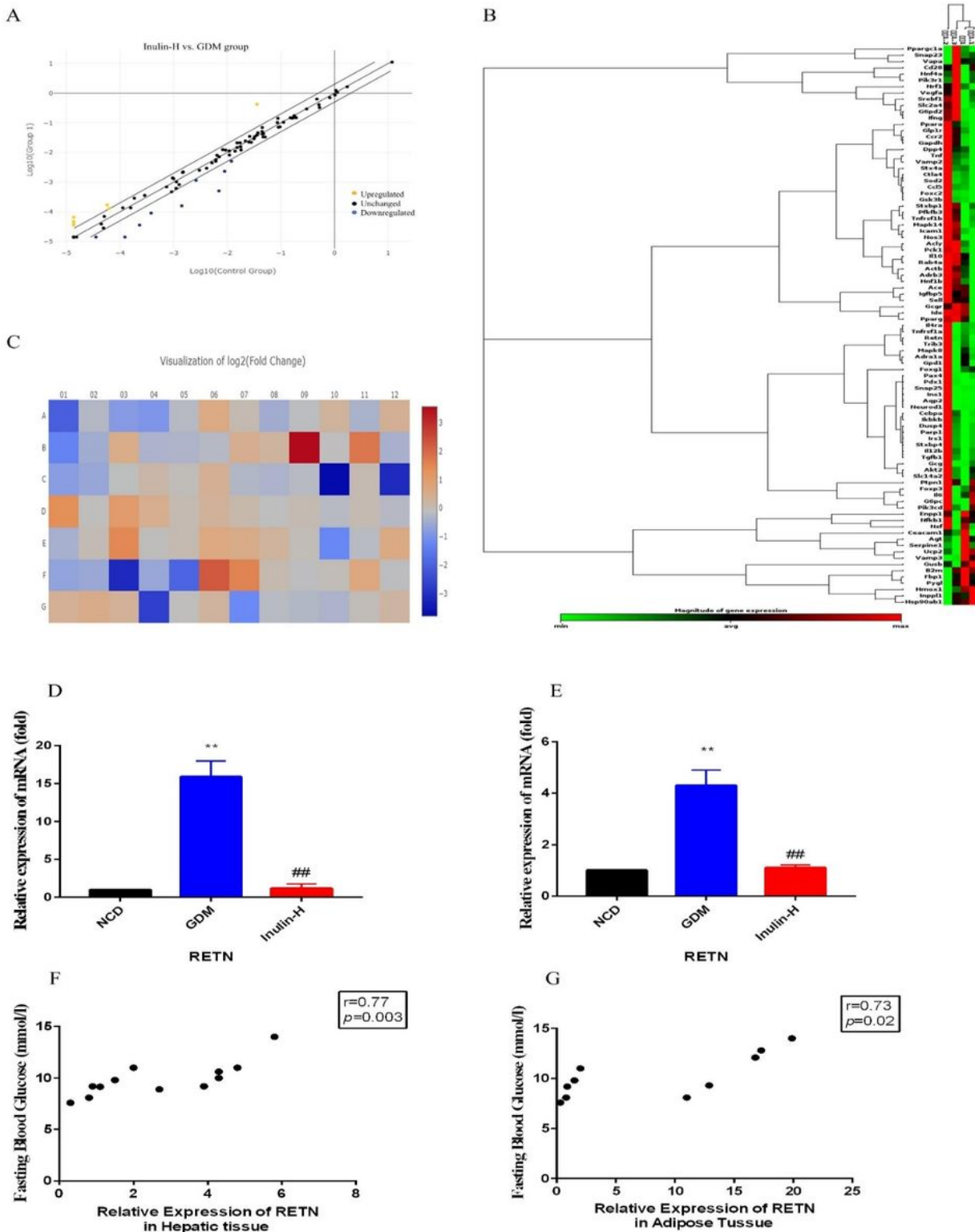


Figure 4

Changes of the candidate genes expressions between GDM and Inulin-H groups by using RT2 profiler PCR array. (A) Scatter plot of the results of every gene expression. The central diagonal line indicates unchanged gene expression, while the outer diagonal lines indicate the selected fold regulation threshold. Yellow dots denote genes with upregulated expression, while blue dots represent genes with downregulated expression. Black dots denote genes with unchanged expression. (B) Cluster gram of

genes with significantly upregulated or downregulated expression. Each column expresses a group, and each row represents a gene. Various colors display the magnitude of gene expression and the degree of gene expression from minimum to maximum is exhibited from green to red. (C) Heat map of the results of every gene expression. Different colors show the different levels of gene expression. Colors ranging from blue to red means downregulated to upregulated gene expression. The most differentially-expressed gene (RETN) validated with qPCR in hepatic (D) and adipose tissues (E). Correlation between RETN expression in hepatic (F) and adipose tissues (G) and fasting glucose levels. Differences were assessed by t-test or Wilcoxon rank-sum test, as appropriate. Correlation analysis was performed with Pearson pairwise test. **P<0.01 vs NCD group; ##P <0.01 vs GDM.

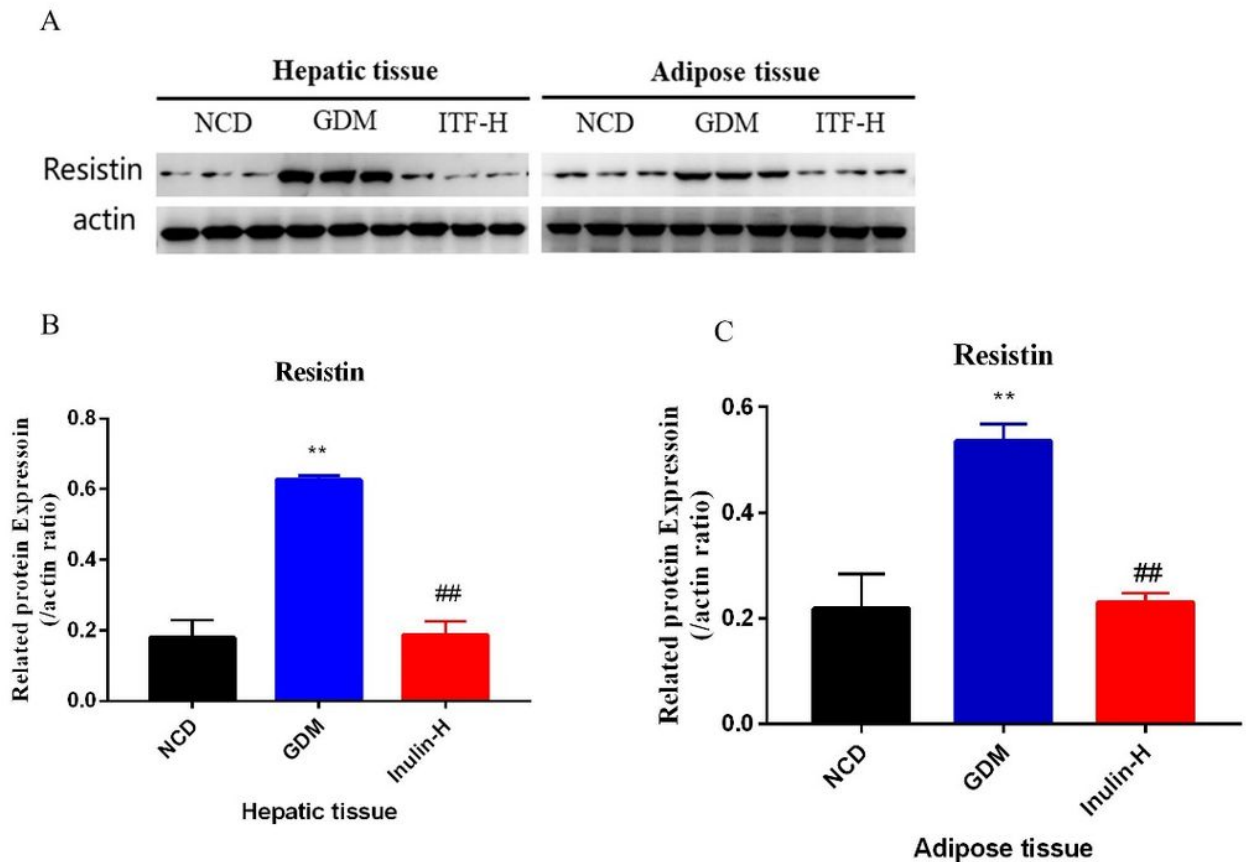


Figure 5

Changes of hepatic and adipose RETN protein expression levels. Representative immunoblot (A) and quantification of RETN (B, C) in the hepatic and adipose tissues of mice from the three groups. Data are expressed as the mean \pm SD values (n = 15). **P<0.01 vs NCD group; ##P <0.01 vs GDM.

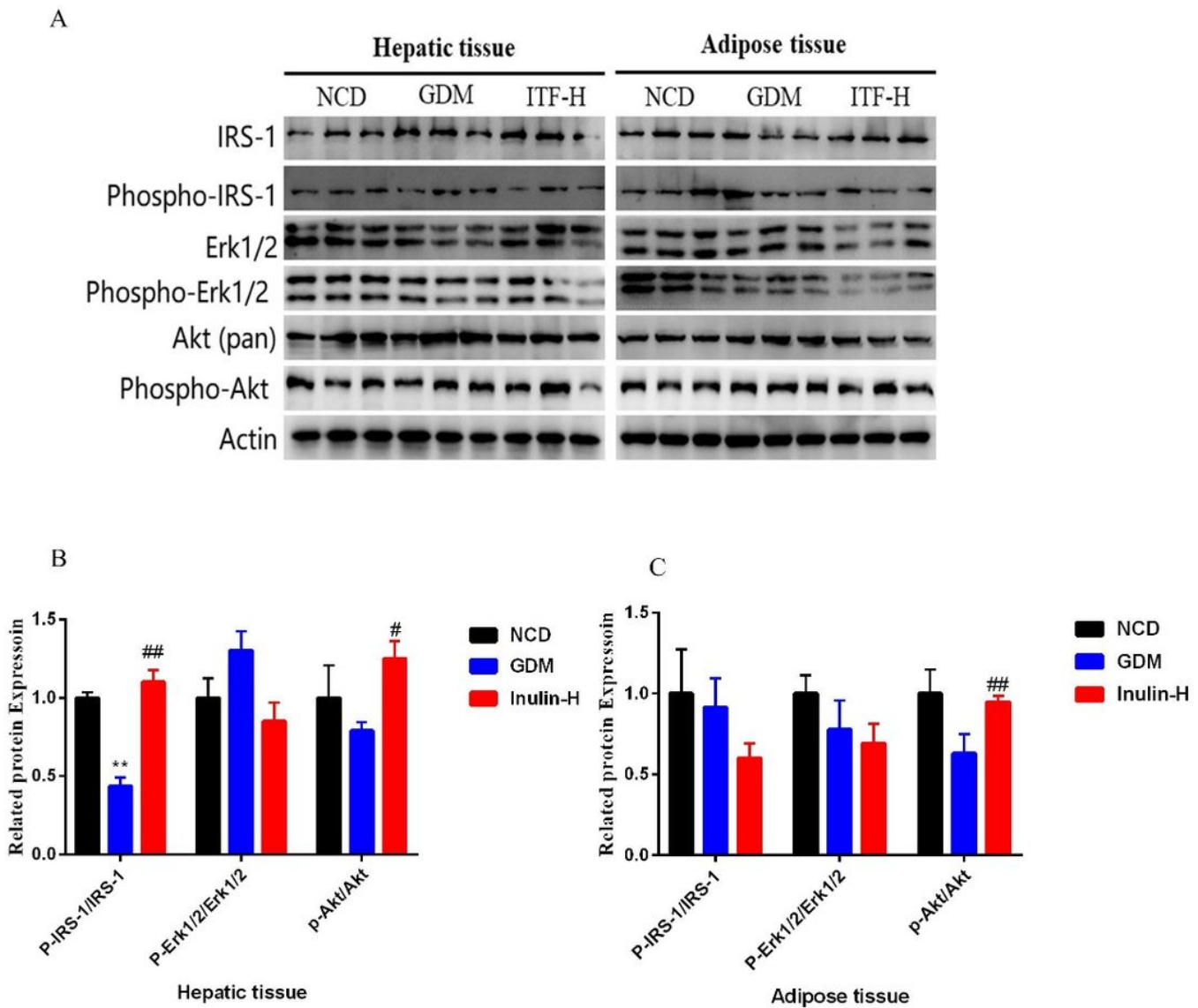


Figure 6

Changes of hepatic and adipose IRS-1, Erk and Akt protein expression levels. Representative immunoblot of IRS-1, p-IRS-1, Erk, p-Erk, Akt and p-Akt in the hepatic and adipose tissues of mice from the three groups (A). The ratios of p-IRS to IRS, Erk to p-Erk and Akt to p-Akt in the hepatic (B) and adipose tissues (C) of mice from the three groups. Data are expressed as the mean \pm SD values (n = 15). **P<0.01 vs NCD group; #P <0.05, ##P <0.01 vs GDM.